Electrodeposition of Nanostructured Mesoporous Selenium Films (H_I-eSe)

Iris Nandhakumar, Joanne M. Elliott,† and George S. Attard*

Department of Chemistry, University of Southampton, Southampton SO17 1BJ, United Kingdom

Received May 17, 2001
Revised Manuscript Received August 18, 2001

We have shown recently that the lyotropic liquid-crystalline phases of polyoxyethylene surfactants can be utilized as versatile nanoscale molds for the formation of highly ordered mesoporous materials such as inorganic oxides and metals.[1−5] In the presence of water the surfactant molecules aggregate into three-dimensional supramolecular assemblies which, at surfactant concentrations greater than ≈30 wt %, spontaneously organize to form lyotropic liquid-crystalline phases. The spatially periodic and orientationally ordered disposition of the surfactant aggregates provides the mold in which the material is formed. In the case of metals or conducting polymers, this is achieved typically by reduction of a suitable precursor dissolved in the aqueous domain of the lyotropic liquid-crystalline phase. Removal of the surfactant affords a material with a porous nanostructure, which is a direct cast of the architecture of the liquid-crystalline phase in which it was formed.[2,3] The range of pore architectures accessible via this route is extensive and is only limited by the lyotropic liquid-crystalline polymorphism of the chosen surfactant/water system. Precise control can be exercised over the nanoarchitecture as well as the pore dimensions, allowing fine-tuning of film properties through suitable choices of surfactants, hydrophobic additives that act as swelling agents, and electrodeposition conditions.[3,4] The nanostructured mesoporous films that are obtained from liquid-crystalline phases combine high specific surface areas and uniform pore structures with mechanical robustness. This combination of properties makes them promising candidates for applications in catalysis, fuel cells, batteries, capacitors, and sensors.[5]

Although electrodeposition from liquid-crystalline phases has been shown to be a generic route to adherent films of nanostructured conducting materials, its use in the production of analogous films of semiconducting materials is not immediately obvious. The ability to electrodeposit semiconducting films that have well-defined mesoporous nanoarchitectures is of relevance for understanding the fundamental physics of low-dimensionality structures and, potentially, for applications in sensors, optical devices, and solar cells. Here, we report that by a careful choice of deposition conditions, it is possible to obtain high-quality films of semiconducting selenium. The electrodeposition of selenium is a particularly challenging test of the versatility of the templating strategy we have developed. This is because selenium can adopt any of four allotropic modifications in its solid state: a vitreous, two monoclinic, and a hexagonal (so-called metallic) phase.[6] The vitreous and monoclinic modifications are insulators. The hexagonal phase of selenium is a semiconductor due to the ordered arrangement of selenium chains facilitating electronic conduction. Because of the solid-state polymorphism of selenium, careful control of electrodeposition conditions (e.g., temperature and current density) as well as careful selection of substrate materials is required to avoid forming the insulating allotropes of the material.

Through a systematic study of the deposition conditions that are required to obtain the semiconducting allotrope of selenium from acidic electroplating baths, it has been shown that the following conditions are essential: a temperature of 100 °C, an electrolyte composed of saturated selenium dioxide in 9 M H_2SO_4, and a deposition current density of up to 0.2 A/cm^2.[6] Under these conditions the deposition of selenium was not accompanied by the discharge of hydrogen ions and the current efficiency was close to 100%. The deposition of mesoporous films of metallic selenium from liquid-crystalline plating mixtures required significant modifications to the electrochemical deposition conditions used in the isotropic systems. This is because the surfactant limits the temperature range and deposition potential as well as the composition and concentration of the components that can be used in the plating mixtures.

In our experiment we employed quaternary plating mixtures prepared from aqueous solutions of 10 mM selenium dioxide dissolved in 2 M sulfuric acid, which were mixed in a 1:1 ratio with 50 wt % of the nonionic surfactant octaethyleneglycol monohexadecyl ether ($C_{16}EO_8$) in deionized water. The optical texture of the plating mixtures was examined under a polarized light optical microscope and reproducibly revealed a normal topology hexagonal mesophase, which was found to be stable up to 72−75 °C. Electrodeposition of the selenium films from the liquid-crystalline plating mixture onto either nickel sheet electrodes (geometric area 1 cm^2), platinum electrodes (cross-sectional areas of 0.002 and 0.008 cm^2) polished with alumina and sealed in glass, or gold on glass films (geometric electrode area of 0.25 cm^2) was carried out under potentiostatic and thermostatic control by stepping the potential from 0 V to between −0.65 and −0.78 V relative to the saturated mercurous sulfate electrode (SMSE) and maintaining a constant temperature of 65 °C. To grow thick visible films of selenium suitable for structural characterization by TEM, XRD, or STM, the potential was stepped from

* To whom correspondence should be addressed. Fax: +44 (0)2380 593019. E-mail: gza@soton.ac.uk.
† Current address: Department of Chemistry, University of Reading, Reading RG6 6AH, UK.

(1) Attard, G. S.; Glyde, J. C.; Göltner, C. G. *Nature* **1995**, *378*, 366.
(2) Attard, G. S.; Göltner. C. G.; Corker, J. M.; Henke, S.; Templer, R. H. *Angew. Chem., Intl. Ed. Engl.* **1997**, *36*, 1315
(3) Attard, G. S.; Bartlett, P. N.; Coleman, N. R. B.; Elliott, J. M.; Owen, J. R.; Wang J. H. *Science* **1997**, *278*, 838.
(4) Elliott, J. M.; Attard, G. S.; Bartlett, P. N.; Coleman, N. R. B.; Merckel, D. A. A.; Owen, J. R. *Chem. Mater.* **1999**, *11*, 3602.
(5) Whitehead, A. H.; Elliott, J. M.; Owen, J. R.; Attard, G. S. *J. Chem. Soc., Chem. Commun.* **1999**, 331.
(6) Hippel, A. V.; Bloom, M. C. *J. Phys. Chem.* **1950**, *18*, 1234.

10.1021/cm010484d CCC: $20.00
Published on Web 09/15/2001

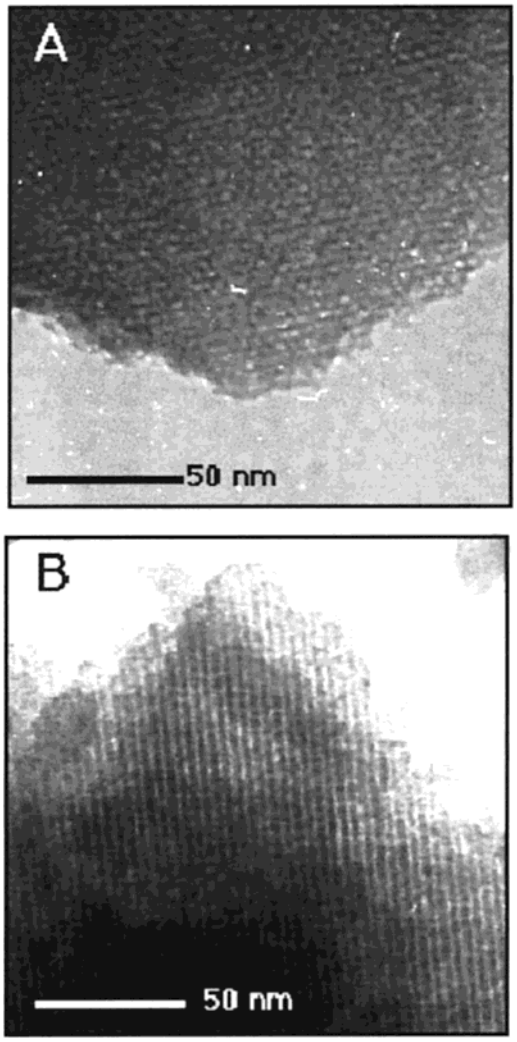

Figure 1. Transmission electron micrographs of selenium electrodeposited at a potential of −0.8 V (vs SMSE) from the hexagonal liquid-crystalline phase of $C_{16}EO_8$ at 65 °C onto a 1-cm^2 nickel sheet electrode: (a) end-on view of pore structure; (b) side view of pores.

0 to −0.65 V vs SMSE with deposition times varying between 3 and 5 h. After deposition, the electrodeposited selenium films (which we denote as H_I-eSe) were allowed to soak in water for at least 24 h. During this period the water was replaced every 2 h until all surfactant was removed. The washed H_I-eSe deposits were typically gray, shiny, and uniform in appearance. Selenium films (denoted by eSe) were also deposited using the same conditions from plating mixtures without surfactant. The eSe films were also gray and shiny.

Transmission electron microscopy was employed to visualize the nanostructure of the H_I-eSe films and this revealed a hexagonal array of cylindrical pores with uniform pore diameter of 25 ± 2 Å (Figure 1). This is comparable with that observed for mesoporous platinum (H_I-ePt) electrodeposited from the H_I phase of the same surfactant.[3] The selenium wall thickness at the point of nearest contact between neighboring pores was found to be 25 ± 2 Å. The H_I-eSe films were investigated by X-ray diffraction (XRD) and scanning tunneling microscopy (STM). Low-angle X-ray diffractograms were characterized by a single broad primary reflection (d_{100}) at 1.52° (2θ), which corresponds to a lattice periodicity of

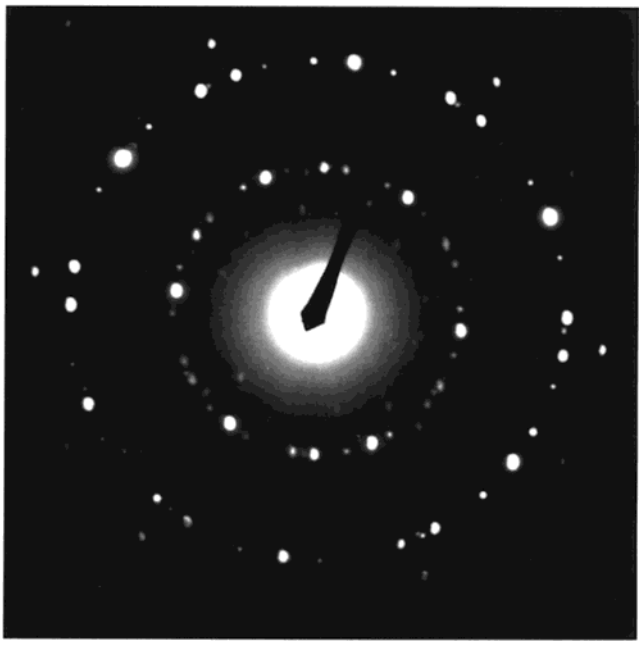

Figure 2. Electron diffraction pattern of H_I-eSe obtained under the conditions described in Figure 1.

58 ± 3 Å and a pore-to-pore distance of 67 Å. This peak was not observed for reference selenium films (eSe) deposited in the absence of surfactant. The presence of only one scattering peak as well as its broad line width are attributed to the dynamic disorder present in the liquid-crystalline phase at elevated temperatures. Selective area diffraction patterns obtained using the transmission electron microscope showed that the walls in H_I-eSe were single crystalline with a hexagonally close-packed (hcp) structure (Figure 2). The most intense diffraction occurred from the $(10\bar{1}2)$ plane, which is consistent with previous X-ray data reported for eSe obtained by electrodeposition from acidic and alkaline solutions ($d_{10\bar{1}2}$ = 2.14 Å for H_I-eSe, compared with 2.0318 Å for Se).[7] STM was employed to record tunneling current versus tunneling bias voltage curves to determine the conductance characteristics of the H_I-eSe deposits. The $I-V$ curves recorded by STM for the nanostructured selenium films in air showed the behavior that they are intrinsic semiconductors with an apparent band gap of ≈1.0 (±0.3) eV.[8]

The H_I-eSe films deposited onto gold on glass electrodes and polished platinum macroelectrodes were analyzed electrochemically by cycling them in solutions of 0.05 M $CdSO_4$ dissolved in 0.1 M sulfuric acid between +0.2 and −0.84 V vs SMSE. A typical cyclic voltammogram is shown in Figure 3. The real surface area as well as surface roughness of the H_I-eSe electrodes were estimated by integrating the currents associated with underpotential deposition (UPD) of cadmium in the forward and reverse potential scans.[9] In our calculations we assumed a conversion factor of 416.7 μC/cm^2 for Cd UPD and subtracted the charge associated with double-layer capacitive charging. We

(7) Zhadanov, S. I. *Encyclopedia of Electrochemistry of the Elements. IV*; Bard, A. J., Ed.; Marcel Dekker: New York, 1975.
(8) Magonov, S. N.; Whangbo, M. H. *Surface Analysis with STM and AFM*; VCH: Weinheim, 1996.
(9) Lister, T. E.; Colletti, L. P.; Stickney, J. L. *Appl. Surf. Sci.* **1996**, *107*, 153.

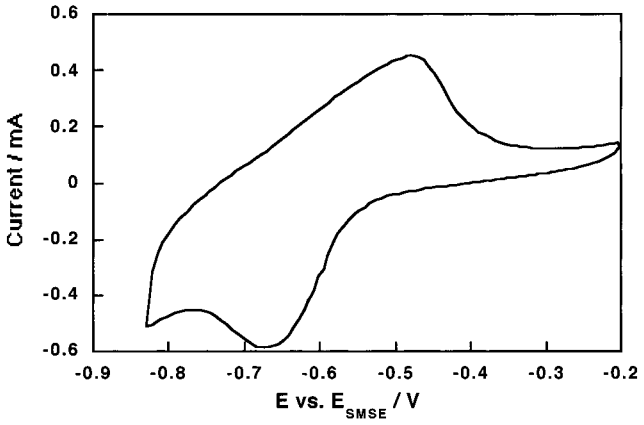

Figure 3. Cyclic voltammogram recorded at a scan rate of 50 mV s^{-1} of the underpotential deposition of cadmium onto an H_I-eSe film deposited at −0.78 V (vs SMSE) at 65 °C onto a 0.25-cm^2 gold on glass electrode. The charge density associated with cadmium deposition was 8.42×10^{-3} C cm^{-2}.

also assumed that Cd forms a uniform monolayer of hexagonally close-packed but unassociated Cd atoms with an interatomic spacing of 2.98 Å (equivalent to that found in the (0001) plane of its hcp bulk structure) with a surface atom density of 1.30×10^{15} atoms cm^{-2}; this is within a factor of 2 of the reported surface atom densities for CdSe monolayers on gold.[10] The scan rate was varied in the range of 20−200 mV s^{-1}. The surface roughness factor for H_I-eSe was found to be 20, while that of eSe deposited under identical conditions was found to be 1−2. It is noted that cadmium UPD on both H_I-eSe and eSe electrodes is characterized by a distinct hysteresis in the potential of the deposition and stripping peaks. This is an indication of a kinetic hindrance in the cadmium adsorption/desorption process and may be a consequence of a first-order phase transition. Such phase transitions are most often associated with nucleation and growth processes; the formation of stable growth centers requires an overpotential that results in a shift between the anodic and cathodic UPD waves.[11]

The ability to produce H_I-eSe films and their post-deposition modification with cadmium suggests that liquid-crystalline plating mixtures could be employed in the production of other elemental semiconductors (e.g., tellurium) as well as II−VI semidconductors (e.g., CdSe, CdTe) and related materials (e.g., PbSe). Because the mesopore diameters and the topology of the nanoarchitecture are under direct experimental control, this novel approach to nanostructured semiconductors affords unique systems in which the relationships between nanoarchitecture and quantum size effects can be explored.

Acknowledgment. This work was funded by the Engineering and Physical Sciences Research Council of the U.K.

Supporting Information Available: Data on the synthesis of nanostructured materials in liquid-crystalline phases and on low-angle X-ray diffraction studies (PDF). This material is available free of charge via the Internet at http://pubs.acs.org.

CM010484D

(10) Lister, T. E.; Colletti, L. P.; Stickney, J. L. *Isr. J. Chem.* **1997**, *37*, 287.

(11) Hölzle, M. H.; Retter, U.; Kolb, D. M. *J. Electroanal. Chem.* **1994**, *371*, 101.